Journal of Alloys and Compounds 507 (2010) 196–200

Contents lists available at ScienceDirect

Journal of Alloys and Compounds

journal homepage: www.elsevier.com/locate/jallcom

Dielectric properties of $(NaBi_{(1-x)}K_x)_{0.5}Ti_{(1-x)}Nb_xO_3$ ceramics fabricated by mechanical alloying

Laijun Liu*, Zhao Yang, Meixia Wu, Liang Fang, Changzheng Hu

State Key Laboratory Breeding Base of Non-ferrous Metal and Characteristic Materials Processing, School of Materials Science and Engineering, Guilin University of Technology, Guilin 541004, China

ARTICLE INFO

Article history:
Received 23 April 2010
Received in revised form 19 July 2010
Accepted 22 July 2010
Available online 30 July 2010

Keywords:
Titanates
Niobates
Dielectric properties
Mechanical alloying technique

ABSTRACT

A/B-site complex perovskite $(NaBi_{(1-x)}K_x)_{0.5}Ti_{(1-x)}Nb_xO_3$ (also can be written: $(1-2x)Na_{0.5}Bi_{0.5}TiO_3$–$xK_{0.5}Bi_{0.5}TiO_3$–$xNaNbO_3$) ($x$ = 0–0.08) lead-free piezoelectric ceramics were fabricated by mechanical alloying technique from their oxide/carbonate mixture. Phase evolvements of the mixture and the influence of x value on crystal structure and microstructure were investigated. The perovskite $Na_{0.5}Bi_{0.5}TiO_3$ phase was progressively formed with passing through the intermediate $Bi_4Ti_3O_{12}$ phases with increasing degree of mechanical activation. The Curie–Weiss law and a modified empirical expression were employed to describe the ferroelectric phase transition of $(NaBi_{(1-x)}K_x)_{0.5}Ti_{(1-x)}Nb_xO_3$ ceramics. The results showed that $(NaBi_{(1-x)}K_x)_{0.5}Ti_{(1-x)}Nb_xO_3$ ceramics became more relaxor ferroelectric characteristic with the increase in value of x. The enhancement of relaxor characteristic may arise from structural disorder and compositional fluctuation in the crystal structure.

1. Introduction

There is an increasing demand for the environment friendly materials like lead-free ceramics for different piezoelectric application fields. Sodium bismuth titanate, $Bi_{0.5}Na_{0.5}TiO_3$ (BNT), is a kind of perovskite (ABO_3-type) ferroelectric discovered by Smlenskii et al. [1]. The dielectric constant of BNT shows a flat, frequency-dependent hump assigned to ferroelectric– anti-ferroelectric phase transition at ~230 °C; as well as the symmetry of BNT changes to cubic symmetry at ~520 °C [2]. Therefore, BNT is considered as an excellent candidate of lead-free piezoelectric ceramics because it is ferroelectric with a relatively large remanent polarization, P_r = 38 μC/cm^2, and a relatively large coercive field, E_c = 7.3 kV/mm [1].

Very recently, a novel mechanical alloying technique has been successfully devised to synthesize a variety of lead-based functional ceramics [3–5]. The intrinsic advantage of mechanical alloying lies in its ability to effect a solid state reaction through mechanical activation, instead of by the calcination at a high enough temperature. It can also lead to an improvement in the reactivity of starting materials and therefore the desired ceramic phase is formed at a lowered calcination temperature. Therefore, mechanical alloying technique may minimize or avoid volatilization of alkaline oxides at high temperatures

Potassium bismuth titanate, $Bi_{0.5}K_{0.5}TiO_3$ (BKT), first discovered by Smolenskii [6], also has a perovskite-type ferroelectric structure belonging to tetragonal crystal system at room temperature. It undergoes a phase transition around 380 °C (Curie point). Ivanova et al. [7] reported the lattice parameters of BKT as a = 3.913 Å and c = 3.990 Å at room temperature. Much work has been done to modify and improve the piezoelectric properties of BNT ceramics by cation substitution [8–16], such as $Bi_{0.5}Na_{0.5}TiO_3$–$SrTiO_3$–$Bi_{0.5}Li_{0.5}TiO_3$ [8], $Bi_{0.5}Na_{0.5}TiO_3$–$SrTiO_3$ [9] and $Bi_{0.5}Na_{0.5}TiO_3$–$BaTiO_3$ [12]. Meanwhile, BNT–BKT solid solutions have been reported to be superior piezoelectric in high-frequency ultrasonic applications with a low dielectric constant and a high electromechanical coupling factor along with a high mechanical strength [17–20]. Niobium doped BNT–BKT is A/B-site complex perovskite compound. Therefore, the structure evolvement and relaxor characteristic of BNT–BKT–niobate solid solutions are very interesting.

In this study, A/B-site complex perovskite ferroelectric, $(NaBi_{(1-x)}K_x)_{0.5}Ti_{(1-x)}Nb_xO_3$ solid solutions were prepared by mechanical alloying technique from their oxide/carbonate mixture. The purpose of this work is to illustrate the phase evolvement of the mixture and the effects of ion substitution on crystal structure evolvement in BNT, as well as to understand the relaxor characteristic of the ternary system.

2. Experimental procedures

Mechanical alloying technique was used to prepare $(NaBi_{(1-x)}K_x)_{0.5}Ti_{(1-x)}Nb_xO_3$, ($x$ = 0, 0.02, 0.04, 0.06, 0.08) solid solutions. Reagent grade oxide or carbonate pow-

* Corresponding author. Tel.: +86 773 5893395.
E-mail address: ljliu2@163.com (L. Liu).

0925-8388/$ – see front matter © 2010 Elsevier B.V. All rights reserved.
doi:10.1016/j.jallcom.2010.07.154

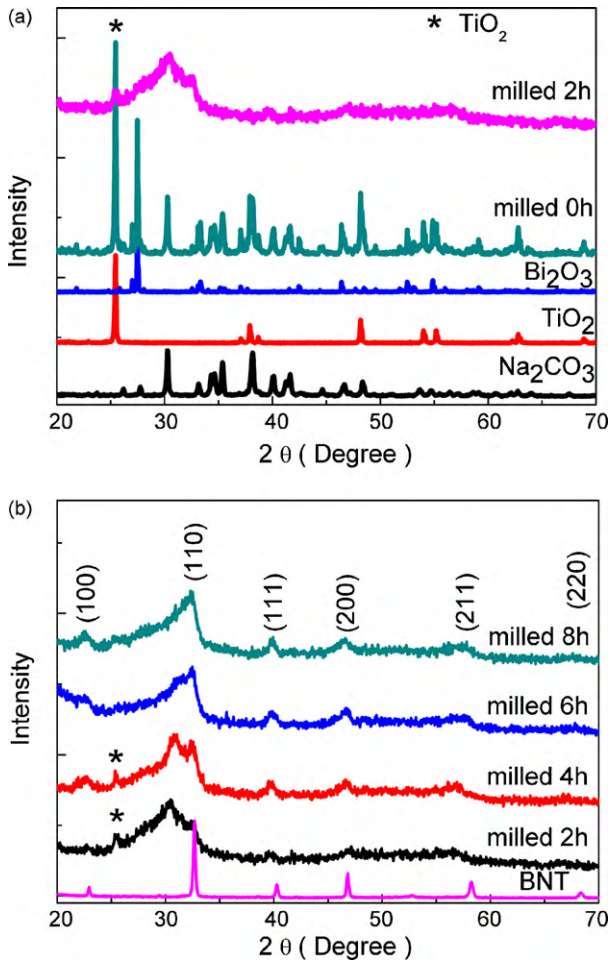

Fig. 1. (a) XRD patterns of Na_2CO_3, K_2CO_3 and TiO_2 and their mixture mechanically activated for 0 h and 2 h; (b) XRD pattern of the mixture mechanically activated for 2–8 h and pure BNT ceramics, indexed based on ICSD-043769.

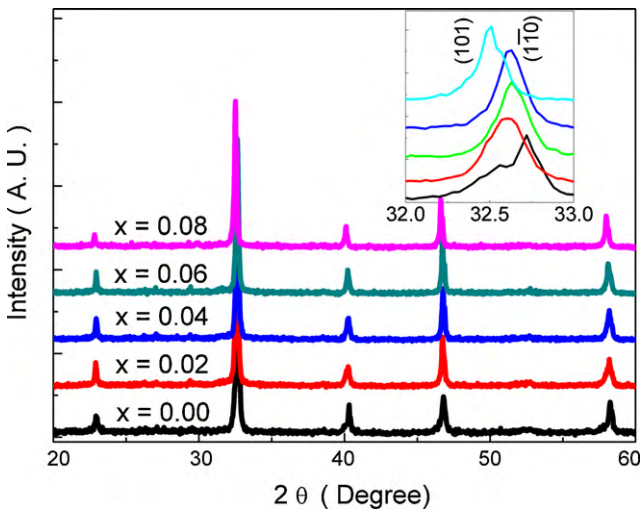

Fig. 2. XRD patterns of $(NaBi_{(1-x)}K_x)_{0.5}Ti_{(1-x)}Nb_xO_3$ ceramics, inset, (1 1 0) peak evolves with the increase in the value of x.

ders of Na_2CO_3, $K_2CO_3 \cdot 1.5H_2O$, Bi_2O_3, TiO_2 and Nb_2O_5 were used as raw materials. The oxides and carbonates were mixed in a planetary mill by ball milling for 0–8 h. After being mixed, the mixture was pressed at 150 MPa into pellets with 20 mm in diameter and about 1.5 mm in thickness. The green compacts were sintered at 1080 °C for 2 h in air atmosphere. Gold had been sputtered on the surfaces of sample as electrodes.

X-ray powder diffraction (XRD) patterns were taken on a PANalytical X'Pert-PRO powder X-ray diffractometer with Cu Kα radiation. Microstructure evolution was studied by scanning electron microscopy (SEM) (JSM-6380LV, JEOL). Relative dielectric constant and loss factor at room temperature and elevated temperature were measured using Agilent 4294A impedance analyzer.

3. Results and discussion

For the sample $(NaBi_{(1-x)}K_x)_{0.5}Ti_{(1-x)}Nb_xO_3$ with $x = 0$, XRD patterns of initial mixture (Na_2CO_3, Bi_2O_3 and TiO_2) and the mixture after milled for 0 h and 2 h are shown in Fig. 1a. After milled

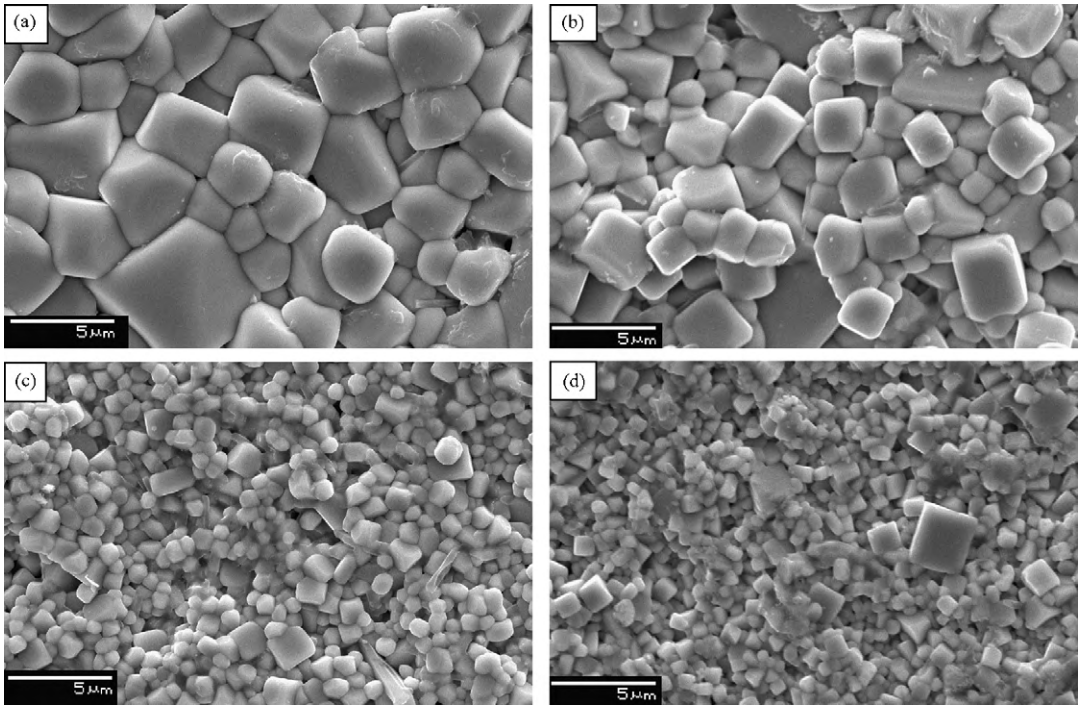

Fig. 3. SEM micrographs of $(NaBi_{(1-x)}K_x)_{0.5}Ti_{(1-x)}Nb_xO_3$ ceramics, (a) $x = 0.02$, (b) $x = 0.04$, (c) $x = 0.06$, (d) $x = 0.08$.

for 2 h, the peaks corresponding to Na_2CO_3 and Bi_2O_3 gradually disappear, whereas those to TiO_2 are still visible. A new broadened peak is observed at $2\theta \approx 30^\circ$ after milled 2 h, which is assigned to the strongest bismuth titanate ($Bi_4Ti_3O_{12}$) peak (1 1 7) [21]. Furthermore, peaks of TiO_2 disappear gradually with the increase in milling time up to 6 h (Fig. 1b). It is noted that the peak near 30° splits into two peaks (Fig. 1b); the first one is attributed by the formation of $Bi_4Ti_3O_{12}$, while the second one, corresponding to the strongest BNT (1 1 0) peak, becomes more and more visible. After milled for 8 h, clear BNT peaks are present without any peaks of secondary phase, which are indexed based on ICSD-043769. Similar results were also found in different x value compounds. It is considered that $Bi_3Ti_4O_{12}$ is obtained firstly in Bi_2O_3–TiO_2–Na_2CO_3 system during mechanical activation, and then sodium ions and titanium diffuse into $Bi_3Ti_4O_{12}$ lattice to become BNT with the increase in milling time. Therefore, the mechanical alloying method is an effective method to yield BNT based compounds starting with oxides and carbonates at room temperature.

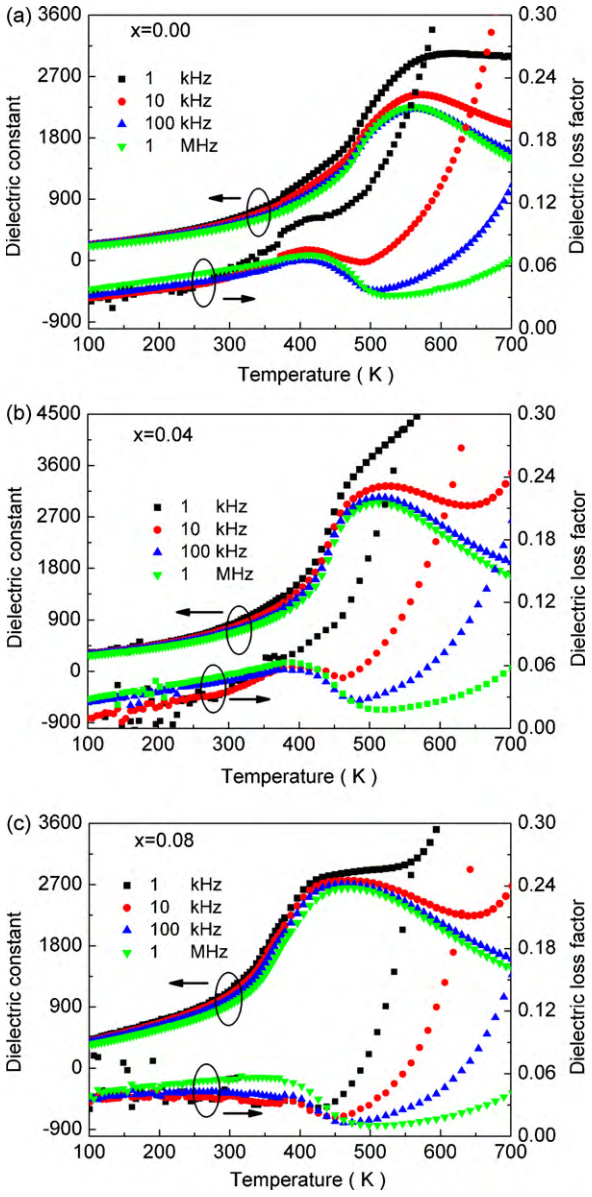

Fig. 4. Dielectric constant and the dielectric loss factor of $(NaBi_{(1-x)}K_x)_{0.5}Ti_{(1-x)}Nb_xO_3$ ceramics as a function of temperatures at 1 kHz, 10 kHz, 100 kHz and 1 MHz. (a) $x = 0.00$, (b) $x = 0.04$, (c) $x = 0.08$.

XRD patterns of $(NaBi_{(1-x)}K_x)_{0.5}Ti_{(1-x)}Nb_xO_3$ ceramics are shown in Fig. 2. All samples belong to pure perovskite structure, yet showing a changing symmetry with the increase in substitution content. No $KNbO_3$ or $NaNbO_3$ peaks are present in XRD patterns. For pure BNT, it displays a typical rhombohedral symmetry at room temperature. However, the crystal structure changes rapidly with the increase in the value of x. The (1 1 0) diffraction peaks of rhombohedral symmetry gradually combine into one broaden peak (not a single peak) of tetragonal symmetry as the amount of the substitution increases. However, the structure transition dependence of x value for $(NaBi_{(1-x)}K_x)_{0.5}Ti_{(1-x)}Nb_xO_3$ solid solutions cannot be identified reliably. Morphtropic phase boundary (MPB) between rhombohedral and tetragonal phase can be found near $x = 0.4$ from XRD patterns. These results are consistent with that of BNT ternary solid solutions [18–20].

Microstructures of $(NaBi_{(1-x)}K_x)_{0.5}Ti_{(1-x)}Nb_xO_3$ ceramics are compared in Fig. 3. It is noticeable that the average grain size of $(NaBi_{(1-x)}K_x)_{0.5}Ti_{(1-x)}Nb_xO_3$ ceramics changes greatly with varying substitution content. For $x = 0.02$, the average grain size is ~3 μm (Fig. 3a), while grain size decreases to ~0.5 μm for the sample with $x = 0.08$ (Fig. 3d). It is difficult to catch the role of sodium/potassium and niobium playing in grain growth; however, one can take note of that not only grain size but also grain morphology was changed significantly. Since titanium is substituted by niobium in $(NaBi_{(1-x)}K_x)_{0.5}Ti_{(1-x)}Nb_xO_3$ system, the differences of ionic radius and valence and electronegativity will worsen the diffusion coefficient of B-site ions in perovskite lattice. Consequently, the grain growth is inhibited with the increase in niobium concentration, which results in the decrease in average grain size and the development of a homogeneous microstructure.

The temperature dependence of the dielectric constant and the dielectric loss factor of $(NaBi_{(1-x)}K_x)_{0.5}Ti_{(1-x)}Nb_xO_3$ between 100 K and 700 K at 1 kHz, 10 kHz, 100 kHz and 1 MHz are shown in Fig. 4.

Table 1
Curie–Weiss temperature (T_0), Curie–Weiss constant (C), temperatures above the dielectric constant follows Curie–Weiss law (T_{cw}), and diffuseness coefficients (γ) for $(NaBi_{(1-x)}K_x)_{0.5}Ti_{(1-x)}Nb_xO_3$ ceramics at 1 MHz.

Composition	$x = 0.00$	$x = 0.02$	$x = 0.04$	$x = 0.06$	$x = 0.08$
T_{max} (K)	561.6	537.2	513.2	489.2	468.2
T_d (K)	417.5	411.1	390.1	378.1	347.0
ε_{max}	2254.3	3001.8	2945.3	2859.3	2652.6
T_0 (K)	431.4	445.4	429.7	430.7	438.5
$C \times 10^5$ (K)	4.0	4.5	4.5	4.3	3.9
T_{cw} (K)	665.1	654.2	654.2	663.2	699.2
$\Delta T_m = T_{cw} - T_{max}$ (K)	103.5	117.0	141.3	174.2	231.0
γ	1.77	1.91	1.92	1.96	1.97

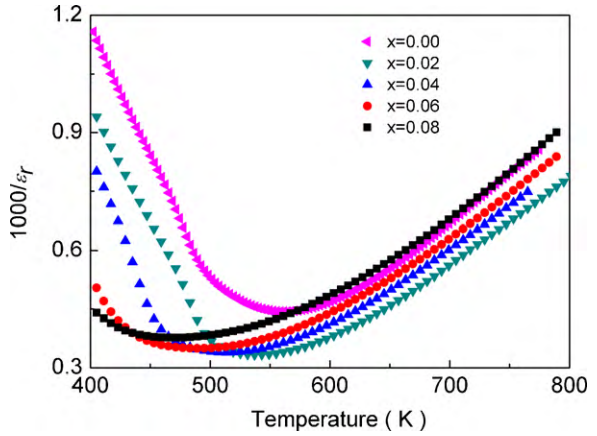

Fig. 5. Inverse dielectric constant ($1000/\varepsilon_r$) as a function of temperature at 1 MHz for $(NaBi_{(1-x)}K_x)_{0.5}Ti_{(1-x)}Nb_xO_3$ ceramics.

It can be evidently seen that there are two dielectric peaks at the temperature range. The two dielectric abnormal peaks can attribute to the reason caused by the phase transitions from ferroelectric to anti-ferroelectric (corresponding to dielectric loss peak) and anti-ferroelectric to paraelectric phase (corresponding to dielectric constant peak), which is consistent with the previous reports of BNT, BNT–$SrTiO_3$, BNT–BKT, BNT–BKT–$KNbO_3$ lead-free ceramics systems [9,12,22,23]. Here, the low transition temperature is called as depolarization temperature (T_d) and the high temperature corresponding to relatively high dielectric constant named as T_m. Both T_d and T_m decrease with the increasing amount of dopants (Table 1).

The dielectric loss peak corresponds to T_d while the dielectric loss factor achieves the minimum value before the temperature T_m. In ferroelectric phase, the dielectric loss factor probably comes from domain wall movement. When phase transition from ferroelectric to anti-ferroelectric occurred at T_d, the domain wall movement enhancement brings to the dielectric loss factor peak. The reason for the disappearance of second dielectric loss factor peak is that the anti-ferroelectric macrodomain would soon break into micro-domains. Above T_m, the sharp dielectric loss factor increase was caused by the high conductivity of ceramics at high temperatures.

It can be also found that all samples have relaxor ferroelectric characteristics. The dielectric constant and dielectric loss factor strongly depend on the measurement frequency. The value of the relative dielectric constant decreases as the measuring frequency

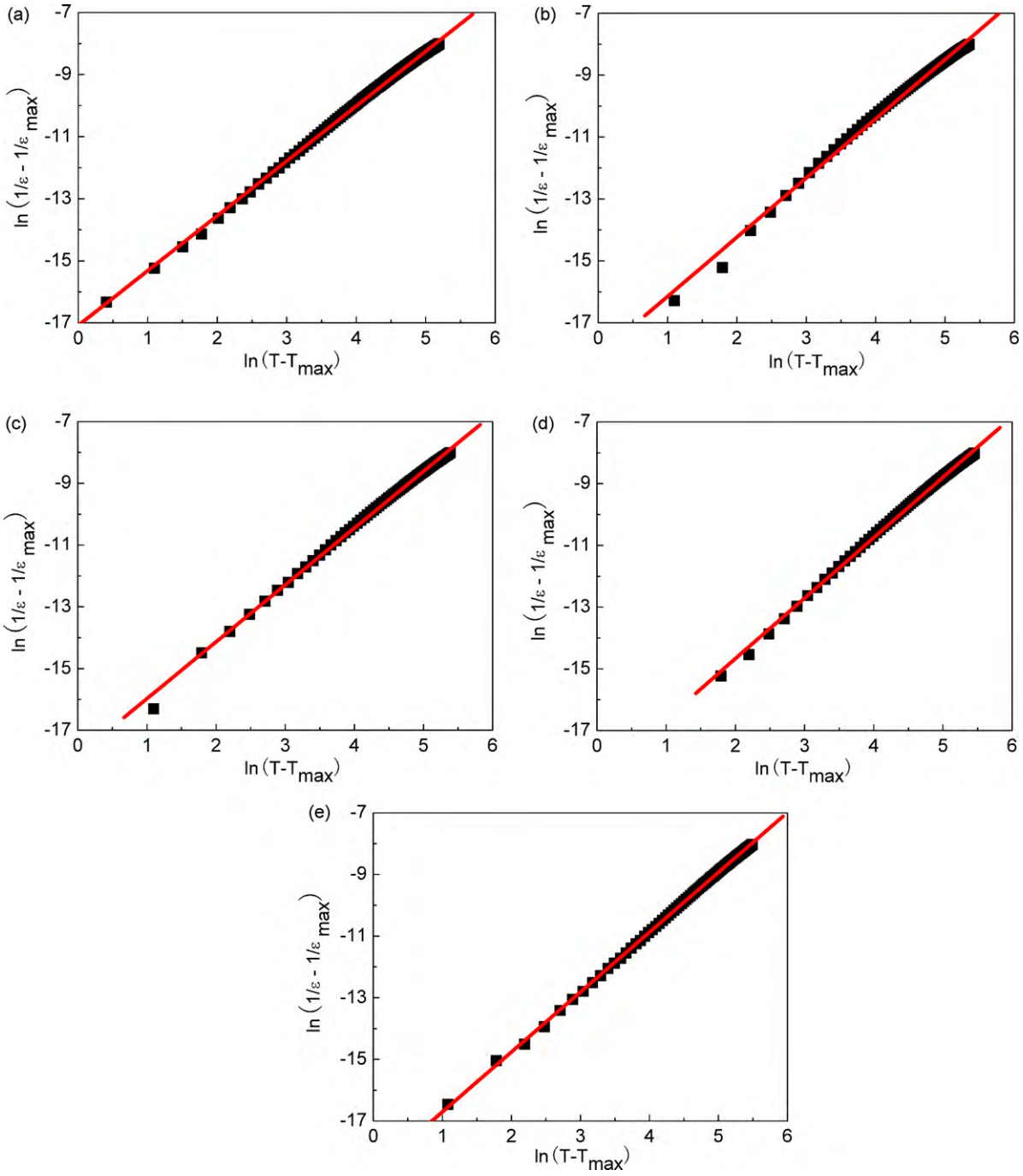

Fig. 6. $\ln(1/\varepsilon - 1/\varepsilon_{max})$ as a function of $\ln(T - T_{max})$ at 1 MHz for $(NaBi_{(1-x)}K_x)_{0.5}Ti_{(1-x)}Nb_xO_3$ ceramics for (a) $x = 0.00$, (b) $x = 0.02$, (c) $x = 0.04$, (d) $x = 0.06$, (e) $x = 0.08$. [The symbols: experimental data; the solid line: fitting to Eq. (3)].

increases. Also, the fact that the dielectric peaks broadening shows the evidence of a diffusion phase transition.

For a normal ferroelectric, dielectric constant above Curie temperature follows the Curie–Weiss law described by:

$$\varepsilon = \frac{C}{T - T_0} \quad (1)$$

where C is Curie–Weiss constant, and T_0 is Curie–Weiss temperature. Fig. 5 shows the inverse of dielectric constant ($1000/\varepsilon_r$) as a function of temperature at 1 MHz. The fitting results obtained by Eq. (1) are listed in Table 1. Deviation from the Curie–Weiss law can be defined by ΔT_m as following:

$$\Delta T_m = T_{cw} - T_{max} \quad (2)$$

where T_{cw} is the temperature at which ε starts to follow the Curie–Weiss law, and T_{max} is the temperature at which ε value reaches the maximum.

Curie–Weiss constant C and ε_{max} increase firstly and then decrease with the increase in the value of x, as well as the peaks of them present in $x = 0.02$. It also can be seen that dielectric constant of $(NaBi_{(1-x)}K_x)_{0.5}Ti_{(1-x)}Nb_xO_3$ ceramics follows the Curie–Weiss law only at temperature much higher than T_{max}. Deviation temperature ΔT_m increases linearly with the increase in the value of x (Table 1). It is suggested that the stability of polar nanoregions (PNR) in $(NaBi_{(1-x)}K_x)_{0.5}Ti_{(1-x)}Nb_xO_3$ ceramics is enhanced with increasing substitution.

A modified empirical expression was proposed by Uchino and Nomura in order to describe the diffusion behavior of ferroelectric phase transition [24]:

$$\frac{1}{\varepsilon} - \frac{1}{\varepsilon_{max}} = C(T - T_{max})^{\gamma} \quad (3)$$

where C and γ are assumed to be constant, with γ value between 1 and 2. The limiting values $\gamma = 1$ and $\gamma = 2$ obey the equation of Curie–Weiss law which are the character for a normal ferroelectric and an ideal relaxor ferroelectric, respectively [25,26].

The values $\ln(1/\varepsilon - 1/\varepsilon_{max})$ were plotted against $\ln(T - T_{max})$ are shown in Fig. 6. A linear relationship is observed for $x = 0$ (Fig. 5a), $x = 0.02$ (Fig. 5b), $x = 0.04$ (Fig. 5c), $x = 0.06$ (Fig. 5d) and $x = 0.08$ (Fig. 5e). The slope of the fitting curves is used to determine γ value, and the obtained γ values vary from 1.77 to 1.97 (Table 1). It is suggested that the $(NaBi_{(1-x)}K_x)_{0.5}Ti_{(1-x)}Nb_xO_3$ solid solutions are more relaxor ferroelectric characteristic with the increase in K^+ and Nb^{5+} concentration.

In $(NaBi_{(1-x)}K_x)_{0.5}Ti_{(1-x)}Nb_xO_3$ solid solution, Na^+, K^+ and Bi^{3+} co-occupy A-site, and Ti^{4+} and Nb^{5+} ions co-occupy B-site of ABO_3 perovskite structure. Therefore, cation disorder in perovskite unit cell gives rise to the stability of PNR, which should be one of reasons for an appearance of relaxor state. In addition, it is known that BNT is a rhombohedral structure and BKT is a tetragonal structure and $NaNbO_3$ shows an orthorhombic structure (anti-ferroelectrics) at room temperature. In this case, macrodomain in pure BNT may be divided into micro-domains with increasing K^+ and Nb^{5+} content, which also may result in an appearance of more relaxor-like behavior.

4. Conclusions

$(NaBi_{(1-x)}K_x)_{0.5}Ti_{(1-x)}Nb_xO_3$ ($0 \le x \le 0.08$) ceramics have been synthesized by using mechanical alloying technique. For $x = 0$ sample, the oxide/carbonate mixture passes through the intermediate $Bi_4Ti_3O_{12}$ phase and then forms BNT with the increase in triggering time. A morphtropic phase boundary between rhombohedral and tetragonal phase could be found near $x = 0.4$ from XRD patterns. Grain size becomes smaller and the morphology of grain undergoes homogenous with the increase in substitution concentration. The relationship between dielectric constant and temperature revealed a diffused phase transitions in the system. $(NaBi_{(1-x)}K_x)_{0.5}Ti_{(1-x)}Nb_xO_3$ ceramics become more relaxor ferroelectric characteristic with the increase in the value of x, which is attributed to structural disorder and compositional fluctuations in BNT lattice.

Acknowledgment

This work was financially supported by the Natural Science Foundation of Guangxi Province (No. 2010GXNSFC013002).

References

[1] G.A. Smlenskii, V.A. Isupv, A.I. Afranovskaya, N.N. Krainik, Sov. Phys. Solid State 2 (1961) 2651.
[2] I.P. Pronin, P.P. Syrnikov, V.A. Isupov, V.M. Egorov, N.V. Zaitseva, Ferroelectrics 25 (1980) 395–397.
[3] J. East, D.C. Sinclair, J. Mater. Sci. Lett. 16 (1997) 422.
[4] Z.F. Zhang, Z.G. Wang, Prog. Mater. Sci. 53 (2008) 1025–1099.
[5] S. Mahboob, G. Prasad, G.S. Kumar, J. Mater. Sci. 42 (2007) 0022–2461.
[6] G.A. Smolenskii, Sov. Phys. Solid State 1 (1959) 1562.
[7] V.V. Ivanova, A.G. Kapyshev, Y.N. Venetsev, V.S. Zhdanov, Izv. Akad. Nauk SSSR, Ser. Fiz. 24 (1962) 354.
[8] D. Lin, K.W. Kwok, H.L.W. Chan, J. Alloys Compd. 481 (2009) 310–315.
[9] Y. Wang, Z. Wang, H. Xu, D. Li, J. Alloys Compd. 484 (2009) 230–232.
[10] M. Liu, D. Yang, Y. Qu, J. Alloys Compd. 496 (2010) 449–453.
[11] J. Shi, W. Yang, J. Alloys Compd. 472 (2009) 267–270.
[12] M. Cernea, E. Andronescu, R. Radu, F. Fochi, C. Galassi, J. Alloys Compd. 490 (2010) 690–694.
[13] Y. Wang, G. Xu, X. Ji, Z. Ren, W. Weng, P. Du, G. Shen, G. Han, J. Alloys Compd. 475 (2009) L25–L30.
[14] Y. Wang, X. Zhao, J. Jiao, Q. Zhang, W. Di, H. Luo, C. Leung, S. Or, J. Alloys Compd. 496 (2010) L4–L6.
[15] Y. Li, R. Liao, X. Jiang, Y. Zhang, J. Alloys Compd. 484 (2009) 961–965.
[16] L. Liu, H. Fan, S. Ke, X. Chen, J. Alloys Compd. 458 (2008) 504–508.
[17] X. Chen, Y. Liao, H. Wang, L. Mao, D. Xiao, J. Zhu, Q. Chen, J. Alloys Compd. 493 (2010) 368–371.
[18] Z. Yang, Y. Hou, H. Pan, Y. Chang, J. Alloys Compd. 480 (2009) 246–253.
[19] C. Zhou, X. Liu, W. Li, C. Yuan, J. Alloys Compd. 478 (2009) 381–385.
[20] M. Zou, H. Fan, L. Chen, W. Yang, J. Alloys Compd. 495 (2010) 280–283.
[21] B.D. Stojanovic, C.O. Paiva-Santos, M. Cilense, C. Jovalekic, Z.Z. Lazarevic, Mater. Res. Bull. 43 (2008) 1743–1753.
[22] S. Said, J.P. Mercurio, J. Eur. Ceram. Soc. 21 (2001) 1333.
[23] Y. Li, W. Chen, Q. Xu, J. Zhou, J. Mater. Sci. 40 (2005) 3625–3628.
[24] K. Uchino, S. Nomura, Ferroelectr. Lett. Sect. 44 (1982) 55–61.
[25] G.A. Smolenskii, A.I. Agranovskaya, Sov. Phys. Tech. Phys. 3 (1958) 1380–1382.
[26] G.A. Smolenskii, Jpn. J. Phys. Soc. 28 (Suppl.) (1970) 26–37.